GEOPHYSICAL RESEARCH LETTERS
December 2005; 32(24) : L24614
http://dx.doi.org/10.1029/2005GL023915

Gyroscopic waves in the Mediterranean Sea

Hans van Haren[1] and Claude Millot[2*]

[1]Royal Netherlands Institute for Sea Research (NIOZ), Den Burg, Netherlands
[2]Antenne LOB-COM-CNRS, La Seyne-sur-mer, France

*: Corresponding author : Claude.Millot@ifremer.fr

Abstract: In the ocean outside areas of dense-water formation, coherent vertical motions (w) are generally much weaker (~10−3) than horizontal (u, v) ones. According to theoretical models based upon "the traditional approximation", i.e. where the horizontal component of the Coriolis force is neglected, describing inertio-gravity waves in the ocean interior, this holds especially for motions at the inertial frequency f: w(f) < O(10−2(u(f),v(f))). We present observations of significant w(f), with mean values of 10−1(u(f),v(f)) and occasional values of 1(u(f),v(f)), from the deep Western Mediterranean Sea characterized by very small buoyancy frequency N = 0 ± 0.4f. Our observations also present evidence of vertical propagation of internal waves, originated in the near-surface density stratified layers, through homogeneous layers below. The observations could be interpreted only within the framework of "non-traditional approach" with the horizontal component of the Coriolis force fully taken into account.

Abstract

In the ocean outside areas of dense-water formation, coherent vertical motions (w) are generally much weaker (~10^{-3}) than horizontal (u, v) ones. According to theoretical models based upon "the traditional approximation", i.e. where the horizontal component of the Coriolis force is neglected, describing inertio-gravity waves in the ocean interior, this holds especially for motions at the inertial frequency f: $w(f)<O(10^{-2}(u(f),v(f)))$. We present observations of significant w(f), with mean values of $10^{-1}(u(f),v(f))$ and occasional values of $1(u(f),v(f))$, from the deep Western Mediterranean Sea characterized by very small buoyancy frequency $N=0\pm0.4f$. Our observations also present evidence of vertical propagation of internal waves, originated in the near-surface density stratified layers, through homogeneous layers below. The observations could be interpreted only within the framework of "non-traditional approximation" with the horizontal component of the Coriolis force fully taken into account.

1. Introduction

Inertial motions are amongst the most energetic motions in large parts of the ocean, with magnitudes comparable to those of tidal currents. Vertical differences in horizontal inertial motions, inertial shear, generally dominate tidal shear due to a smaller vertical length scale linked to the vertical stratification in density. As a result, inertial motions are important for deep-ocean mixing. As stratification can support internal (inertio-)gravity waves, commonly used theories based on the traditional approximation predict propagating waves at *super*-inertial frequencies. At f, pure oscillations can exist that do not propagate but are rapidly damped by (bottom) friction. For weakly stratified waters, the non-traditional approximation, considering the horizontal component of the Earth's rotational vector, predicts propagating inertio-gravity waves (or gyroscopic waves in homogeneous water), also at *sub*-inertial frequencies, and propagating inertio-gravity waves are predicted at f [*LeBlond and Mysak,* 1978*; Gerkema and Shrira,* 2005]. Although such waves are characterised by relatively large w(f) values $O(10^{-1}\text{-}1\cdot(u(f), v(f)))$, they have never been observed in situ up to now. Here we show such w(f) values in recent acoustic Doppler current profiler (ADCP) observations from a deep layer that is nearly-homogeneous as far as can be measured by today's instruments.

Inertial motions are mainly generated near the surface by temporal variability in wind stress, due to the Coriolis effect of the rotating Earth [e.g. *Webster*, 1968; *Perkins*, 1972; *Millot and Crépon*, 1981; *Garrett*, 2001]. However, enhanced near-inertial energy can be found in the deep [*Fu*, 1981; *Saunders*, 1983; *van Haren et al.*, 2002], suggesting possible generation near the bottom due to relaxation of fronts as hypothesised for surface waters [*Tandon and Garrett*, 1995], downward energy propagation via fronts [*Davies and Xing*, 2004] or accumulation of canonical [*Garrett and Munk*, 1972; GM] internal waves encountering their turning latitude [*Fu*, 1981]. In the absence of (relaxing) fronts, the latter model may explain a 7 dB elevation of near-inertial energy above the background spectral level for a mid-latitude ocean, but it cannot explain the observations presented here because *i*) the observed near-inertial spectral peak is 13-20 dB above the background level, *ii*) the Western Mediterranean Sea extends only ~600 km in meridian direction (equivalent to ±6% variation in f), which is a very small portion of the GM spectrum, and *iii*) the downward propagating motions have to pass substantial layers O(100 m) of truly neutral stability that do not support internal gravity waves [*van Haren and Millot*, 2004]. Hence, local near-surface generation is more likely [*Fu*, 1981], which is plausible given the strong pulse-like winds from the north that generate near-surface inertial motions in the whole sea [*Millot and Crépon*, 1981], and we hypothesise deep-sea propagation through homogeneous and well-stratified layers using the non-traditional approximation, focusing on gyroscopic waves.

2. Inertio-gravity waves

Under the traditional approximation, using only the component $f = 2\Omega\sin\varphi$ of the Earth's rotational vector Ω at latitude φ, internal gravity waves can exist at frequencies (σ) in the range $f<\sigma<N = (-g/\rho\ \partial\rho/\partial z)^{0.5}$, g the acceleration of gravity and z denoting the vertical coordinate, for N>f. The extreme frequencies theoretically identify purely horizontal motions having infinitely long wavelengths (f) and purely vertical motions (N). Free waves are predicted to propagate along characteristics $\xi_{\pm}=(dz/d\chi)\chi-z$ in planes (χ, z), where the horizontal coordinate $\chi=x\cos\alpha+y\sin\alpha$, α the angle with respect to the East, positive x-direction (y is positive to the North), that are inclined to the vertical [*LeBlond and Mysak*, 1978],

$$\frac{dz}{d\chi}=\pm\left(\frac{\sigma^2-f^2}{N^2-\sigma^2}\right)^{1/2}, \tag{1}$$

so that for σ=1.02f and N=10f w/v ≈ 0.02 (also for σ=0.99985f when N=0.5f), whilst w(f)=0. However, following (1) no possibility exists for a transfer between sub- and super-inertial motions (e.g. across an interface separating homogeneous and stratified waters). As in the deep ocean N can become so small that it approaches f, a complete reflection is predicted of free inertial waves generated near the surface encountering layers where N=f [*Munk*, 1981].

In contrast, the non-traditional approximation [*Saint-Guily*, 1970; *LeBlond and Mysak*, 1978; *Gerkema and Shrira*, 2005] takes into account $f_h = 2\Omega\cos\varphi$ and the complete set of linear terms in momentum equations. This results in extension of the range [f, N] to [σ_{min}<f, σ_{max}>N], with the *smallest* scale motions at σ_{min}. For N = 0, the wave band is in the range [0, 2Ω]. As f < 2Ω, inertial motions can thus propagate as free waves in homogeneous waters. Under an f-plane approximation the non-traditional internal wave propagation is described for every N by [*Badulin et al.,* 1991; *Gerkema and Shrira*, 2005]:

$$\frac{dz}{d\chi}=\frac{ff_s\pm(f^2f_s^2+(\sigma^2-f^2)(N^2-\sigma^2+f_s^2))^{1/2}}{N^2-\sigma^2+f_s^2}, \tag{2}$$

where $f_s=f_h\sin\alpha$. The two solutions in (2) (or $\xi_{\pm}$) can have very different slopes, whilst the two solutions in (1) are identical. This holds for any α, except for waves propagating in the East-West (x, zonal, α=0, π) direction or for large N>>f for which (2) approaches (1).

From (2) one can expect vertically steep f-energy propagation and thus a large ratio |w(f)|/|u(f)|, |v(f)| (as well as w(f)=0, with large u, v, due to horizontal slopes for the second solution!) for waves propagating in North-South (y, meridian, $\alpha=\pi/2$, $3\pi/2$) direction, also in weak stratification ($N\approx 0<f$).

As the particle motion of f-waves is always circular in their plane of energy propagation and as this plane varies its angle to the vertical depending on N and α (and φ), horizontal f-motions describe a clockwise-polarised ellipse having a polarization expressed as an eccentricity (E) ranging between near-circular (E = 1) and near-rectilinear (E = 0) when projected on the x, y plane [*van Haren and Millot*, 2004] (the two extremes are found for meridian propagation). Energy propagation is in the direction of the minor axis. When the horizontal current describes a nearly rectilinear ellipse at f, a relatively large vertical current w(f) is expected, which does not exist in traditional theory.

So far, gyroscopic waves were only observed in the laboratory [*Oser*, 1958; *McEwan*, 1970; *Manders and Maas*, 2003]. Recently, [*van Haren and Millot*, 2004] extensively described ellipse properties of near-inertial horizontal current meter observations. These ellipse properties varied strongly with time and across the vertical in the Western Mediterranean Sea (vertical currents were not available). These variations suggested a smooth transition of inertio-gravity waves through layers where N changed from near-zero to a non-zero value >f. To provide further evidence of the above, we deployed at the same site a four-beam 75 kHz ADCP to investigate w(f) and vertical propagation of phase, which is opposed to energy propagation in the vertical for N>f but, due to a sign change in the denominator in (2), identical (up or down) for N=0 when $\alpha < \mathrm{asin}(\tan(\varphi))$, ≈ 53° in our area.

3. Data and background conditions

The upward-looking ADCP was moored (together with a thermistor string that did not function correctly) to the southwest of Sardinia in the Algerian sub-basin of the Western Mediterranean Sea (Table 1). The ADCP was set in a 400 kg net buoyancy elliptical float at a depth of ~2400 m, because it was expected to range ~500 m and because the upper limit of the deep homogeneous layer was previously found at ~2200 m (from CTD observations in 1997 and 2001).

Unfortunately, only a range of 200-250 m of permanently good data was realized, due to low amounts of scatterers. In addition, the homogeneous layer, which corresponds to a water mass formed in the north of the Western Mediterranean Sea in winter, was thicker than expected during at least part of the experiment. Its upper limit was at ~1900 m in September 2004 (Fig. 1, upper right panel). Using a Sea-Bird SBE 911*plus* CTD, sampling at 24 Hz temperature accurate to within 10^{-3} °C and conductivity to within $3\cdot10^{-4}$ Sm^{-1}, we estimated $N = 0$ to within an uncertainty of 0.4f in the layer below 1900 m. This uncertainty was ~half due to instrumental errors and ~half due to the imperfect estimation of the adiabatic lapse rate. Although the circulation of this (nearly) homogeneous water was known to be significant [*Millot*, 1999], such a variation in its upper limit was not expected. The ~1900 m limit corresponds to the depth of the channel of Sardinia so that dense water "in excess" in the Algerian sub-basin is expected to outflow into the Tyrrhenian sub-basin (the 2004 situation). A limit at ~2200 m (the 1997 and 2001 situations) is indicative of a dense water "deficit". Above the deep layer of $N = 0$, a ~500-m thick layer of very constant stratification ($N = 2.5\pm0.5f$) is found during both the former and the recent experiments. Although the limit between the two layers varied with time, we expect the 200-250 m range of the ADCP mostly in the homogeneous layer (which is supported by the similarity of the currents over the vertical).

The large buoyancy caused very little mooring motion, as evidenced from pressure and tilt sensor information: variations were <2 m in the vertical or <2.5° tilt angle. The thermistor string did not affect the ADCP's current measurements, as was verified by inspecting the acoustic backscatter records, confirming previous [*Schott*, 1988] experiments with a similar thermistor string mounted in a 75 kHz ADCP beam. As a result, good quality w-data were expected to an accuracy of $3\cdot10^{-4}$ m s^{-1} at f, as the inertial period is ~80 times the ensemble period (for which error is given in Table 1). This quality was further verified using the additional 'error velocity (err)' parameter, defined [*RD Instruments*, 1999] as the difference between two estimates of w computed from the two beam pairs and multiplied by a proper scaling factor [*van Haren et al.*, 1994] for comparison with w. Horizontal and vertical current inhomogeneity, for example caused by an object obstructing one or more beams, affect vertical current measurements when err → w. However, w(f) is significantly measured here because $|w(f)|^2 > 10|err(f)|^2$ as observed below 2200 m (Fig. 1, upper left panel), and the main source of the small error in w(f) is instrumental noise.

4. Observations

Inertial kinetic energy $P_{KE}(f)$ dominates spectra (Fig. 1 upper left panel) even though $N=0\pm0.4f < f$ (Fig. 1 upper right panel). The peak at f has a finite width, which yields the familiar intermittency [*Fu*, 1981] visible in the depth-time plots of band-pass filtered near-inertial motions (Fig. 1 middle panels; v gives a similar picture as u). Bands of large f-current amplitude extend vertically across most of the 480-m range, despite the often bad return above ~2200 m. Note that the intermittency of near-inertial u (or v) and w vary quasi-independently, so that they sometimes show simultaneous large (or small) amplitudes and sometimes opposing in(de)creases in amplitude. As a result, the ratio $|w(f)|/|u(f)|$ varies strongly with time. This variability cannot be attributed to motions forced by bottom slopes, which would yield w in(de)creasing with u or a constant amplitude ratio, besides a relatively low one of ~0.05 (the average bottom slope towards Sardinia). The observed variability is a property of inertio-gravity waves since the two solutions of (2) are very different and any variations in f-motions' source may result in a different response, due to dependence of N,α.

The detail depth-time plot of u(f) (Fig. 1 lowest panel) shows downward propagation of phase. For $N=0$, $\alpha<53°$ this implies downward energy propagation. The weak vertical slanting of 45±45°/300 m points at relatively large vertical phase speeds of ~2400±2400 m/inertial period. Downward phase propagation occurred most of the time (>90%), but the slope varied. However, most conspicuous are the w-observations: w is non-zero with a peak at f (Fig. 1).

Such a peak is absent in the error velocity ('err') spectrum, which represents white noise. In the good-data range, err(f) is at least one order of magnitude less energetic than w(f) and equal to the manufacturer's error estimate, which is also found in w for σ>10 cpd. Thus, the observed w(f) are significant within the 95% level. In the overall mean the ratio $|w(f)|/|u(f)| = 0.12 \pm 0.05$, with periods when w approaches u (Fig. 1 middle panels).

This variation with time is clearly seen in the detail example in Fig. 1. Between days 286-294 $|w(f)|/|u(f)| \rightarrow 1$ is found for depths between 2050-2200 m, whilst the ratio approaches the overall mean value towards day 298. Below 2200 m the mean $|w(f)|/|u(f)| = 0.35 \pm 0.1$ for this 14 day period. These values, including the overall mean of 0.12, are all far too large to be explained using the traditional approximation. A ratio of $|w|/|u| \approx 0.35$ implies a (19° to the vertical) inclined circular motion that is observed as a horizontal current with $E \approx 0.94$ (the mean value observed at ~2350 m), whilst $|w|/|u| = 1.0$ (inclination of 45°) gives $E \approx 0.7$ (the mean value observed at ~2200 m). These E(f) conform to (2) for near-inertial gyroscopic waves (N=0) when the propagation is nearly zonal ($\alpha \approx \pm 8$, 19 (+180)°, respectively), as was observed. Variability in E has further been demonstrated in hodographs in [*van Haren and Millot*, 2004]. E's variability with depth and time, like that of $|w|/|u|$, reflects local variations in relative importance of the two solutions in (2), as a function of variations in near-inertial sources in the layers above and as a function of frontal variability.

5. Discussion

We hypothesize that near-inertial inertio-gravity waves were generated near the surface, as propagation was downward, and in the detailed example in Fig. 1 more or less east-west ($\alpha \approx 8° < 53°$). Then we expect from (2) in the layer N=2.5f $|w(f)|/|u(f)| \approx 0.07$, instead of 0 expected from (1), down to 1900 m, compared to 0.36 observed (in N=0). Unfortunately, the above change in values is not observed. In the near-homogeneous layer energy sometimes increases towards the bottom, evidence of gyroscopic wave trapping, as suggested theoretically [*Gerkema and Shrira*, 2005], but certainly not decreasing exponentially as expected for gravity waves [*Munk*, 1981].

As near-inertial gyroscopic waves have propagation directions that are markedly differ from those of internal gravity waves, we expect distinctly different properties of vertical transport (due to the possibility of much larger w) and deep-ocean mixing (due to their shear magnitude that much more rapidly varies with time). Details of the suggested transfer between stratified and homogeneous layers are yet to be verified. However, observational evidence is given here of near-inertial gyroscopic waves, i.e. internal waves in truly homogeneous water $N=0$, estimated better than $0.4f$, that have not been observed in the ocean before. The observed mean ratio w/u is of the same order as found for sub-inertial motions in restricted areas of deep-water formation [*Voorhis and Webb*, 1970; *Gascard*, 1973], but here the motions are at f so that we deal with $|w(f)|/|u(f)| \approx 0.1$.

Acknowledgments. We thank the crews of the R/V l'Europe and Thethys II for deploying and recovering the 'GYROSCOP' mooring. Gilles Rougier and Theo Hillebrand prepared the mooring and instrumentation. We appreciated the thorough comments of two anonymous referees. We gratefully acknowledge support from the Netherlands organisation for the advancement of scientific research, NWO, and Centre National de la Recherche Scientifique, CNRS, to continue our French-Dutch collaboration.

REFERENCES

Badulin, S.I., V.M. Vasilenko, and M.I. Yaremchuk (1991), Interpretation of quasi-inertial motions using Megapoligon data as an example, *Izv., Atmos. Oc. Phys., 27*, 446-452.

Davies, A. M. and J. Xing (2004), Wind-induced motion in the vicinity of a bottom density front: response to forcing frequency, *J. Geophys. Res., C109* (C09002), doi:10.1029/2003JC002151.

Fu, L.-L. (1981), Observation and models of inertial waves in the deep ocean, *Rev. Geophys. Space Phys., 19*, 141-170.

Garrett, C. (2001), What is the “Near-Inertial” band and why is it different from the rest of the internal wave spectrum? *J. Phys. Oceanogr., 31*, 962-971.

Garrett, C.J.R. and W.H. Munk (1972), Space-time scales of internal waves, *Geophys. Fluid Dyn., 3*, 225-264.

Gascard, J.-C. (1973), Vertical motions in a region of deep water formation, *Deep-Sea Res., 20*, 1011-1027.

Gerkema, T., and V.I. Shrira (2005), Near-inertial waves in the ocean: beyond the “traditional approximation”*, J. Fluid Mech.*, 529, 195-219.

LeBlond, P.H., and L.A. Mysak (1978), *Waves in the Ocean*, 602 pp., Elsevier, New York.

Manders, A.M., and L.R.M. Maas (2003), Observations of inertial waves in a rectangular basin with one sloping boundary*, J. Fluid Mech.*, 493, 59-88.

McEwan, A.D. (1970), Inertial oscillations in a rotating fluid cylinder*, J. Fluid Mech.*, 40, 603-640.

Millot C. (1999), Circulation in the Western Mediterranean sea, *J. Mar. Sys., 20*, 423-442.

Millot, C., and M. Crépon (1981), Inertial oscillations on the continental shelf of the Gulf of Lions-Observations and theory, *J. Phys. Oceanogr., 11*, 639-657.

Munk, W. (1981), Internal waves and small-scale processes, in *Evolution of Physical Oceanography*, edited by B.A. Warren and C. Wunsch, 264-291, MIT, Cambridge, MA.

Oser, H. (1958), Experimentelle Untersuchung über harmonische Schwingungen in rotierenden Flüssigkeiten, *Z. Angew. Math. Mech., 38*, 386-391.

Perkins, H. (1972), Inertial oscillations in the Mediterranean. *Deep-Sea Res., 19*, 289-296.

RD Instruments (1999), *Technical Manual LongRanger ADCP*, RD Instruments, 172 pp., San Diego, CA.

Saint-Guily, B. (1970), On internal waves. Effects of the horizontal component of the Earth's rotation and of a uniform current, *Dt. Hyd. Z.*, *23*, 16-23.

Saunders, P.M. (1983), Benthic observations on the Madeira abyssal plain: currents and dispersion, *J. Phys. Oceanogr.*, *13*, 1416-1429.

Schott, F. (1988), Effects of a thermistor string mounted between the acoustic beams of an acoustic Doppler current profiler, *J. Atmos. Ocean Tech., 5*, 154-159.

Tandon, A. and C. Garrett (1995), Geostrophic adjustment and restratification of a mixed layer with horizontal gradients above a stratified layer, *J. Phys. Oceanogr.*, *25*,2229-2241.

van Haren, H. and C. Millot (2004), Rectilinear and circular inertial motions in the Western Mediterranean Sea, *Deep-Sea Res. I, 51*, 1441-1455.

van Haren, H., N. Oakey and C. Garrett (1994), Measurements of internal wave band eddy fluxes above a sloping bottom, *J. Mar. Res., 52*, 909-946.

van Haren , H., L. Maas, and H. van Aken (2002), On the nature of internal wave spectra near a continental slope, *Geophys. Res. Lett., 29(12)*, 10.1029/2001GL014341.

Voorhis, A.D. and D.C. Webb (1970), Large vertical currents observed in a winter sinking region of the northwestern Mediterranean, *Cah. océanogr., 22*, 571-580.

Webster, F. (1968), Observation of inertial period motions in the deep sea, *Rev. Geophys., 6*, 473-490.

Table 1. ADCP mooring details. Frequency is in cycles per day (1 cpd = $2\pi/86400\ s^{-1}$).

Latitude	38° 26.967′ N
Longitude	007° 39.883′ E
Waterdepth	2840 m
f, period T_f	1.2466 cpd, 19.3 h
Deployment	03/10/2003
Recovery	08/09/2004
ADCP	RDI 75 kHz Longranger (‘Narrow’, HP)
Beam spread	20°
Instrument depth	2428 m
First bin	2395 m
# bins x bin size	60 x 8 m
Ensemble period	900 s
Std u,v	$1.1\cdot10^{-2}$ m s^{-1} /ens
Std w,err	$0.28\cdot10^{-2}$ m s^{-1} /ens
Local stratification N	0±0.5 cpd

Figure 1. Upper left panel shows spectra in 10^{-4} m^2s^{-2}/cpd *i*) at 2370 m: kinetic energy (KE; black), vertical velocity^2 (w; dark-blue) and error velocity^2 (err; green), *ii*) horizontal current difference^2 between 2210 and 2370 m (ΔU; red), *iii*) vertical velocity^2 (w; light-blue) at 2180 m (representing the upper range of good data). Upper right panel shows the density anomaly profile (referenced to 2000 m) obtained in September 2004. The ADCP range is given to the left, with continuous good data in green. The purple lines indicate density stratification yielding N = 0, 2f (solid lines) and N = f, 3f (dashed lines). The two middle panels show the entire depth-time series of near-inertial ADCP-data (band-pass filtered between 0.9-1.1f) for w (multiplied by 10) and u, using the same colors, which are specified in the lowest panel. The horizontal bars indicate the detail period shown in the lower two panels, in which the inertial periodicity is visible (a maximum every 19.3 h). The horizontal white line indicates the approximate depth below which in general good data were obtained.

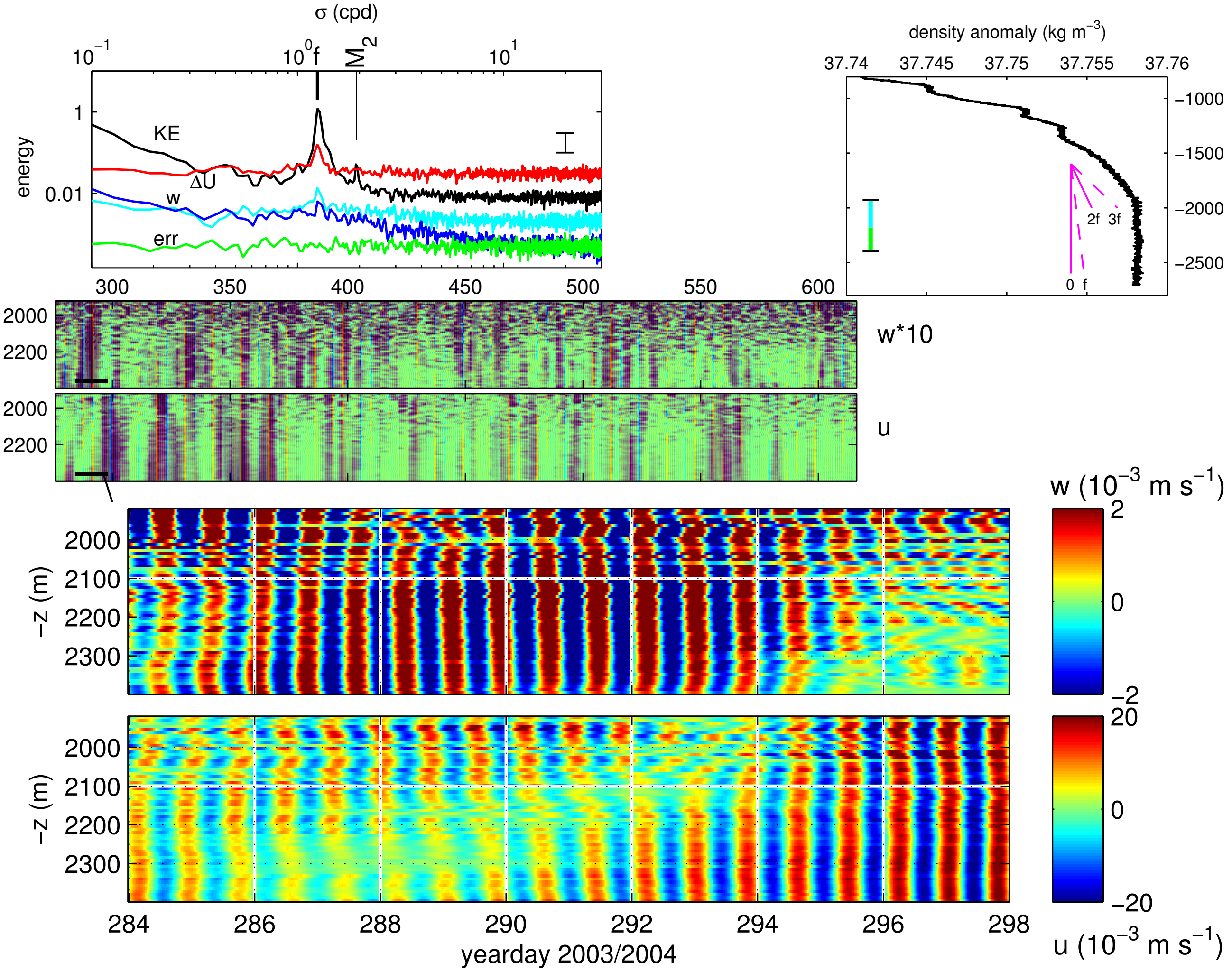
σ (cpd)
10^{-1}
10^{0} f
M_2
10^{1}
energy
1
0.01
KE
ΔU
w
err
300
350
400
450
500
550
600
density anomaly (kg m^{-3})
37.74
37.745
37.75
37.755
37.76
−1000
−1500
−2000
−2500
z (m)
2f
3f
0
f
−z (m)
2000
2200
w*10
u
w (10^{-3} m s^{-1})
2
0
−2
2100
2300
20
−20
284
286
288
290
292
294
296
298
yearday 2003/2004
u (10^{-3} m s^{-1})